Sciencexpress Report

Evidence for Deep Magma Injection Beneath Lake Tahoe, Nevada-California

Kenneth D. Smith,[1*] David von Seggern,[1] Geoffrey Blewitt,[1,2] Leiph Preston,[1] John G. Anderson,[1] Brian P. Wernicke,[3] James L. Davis[4]

[1]Nevada Seismological Laboratory, University of Nevada Reno, Reno, NV 89557, USA. [2]Nevada Bureau of Mines & Geology, University of Nevada, Reno, NV 89557, [3]Division of Geological and Planetary Sciences, California Institute of Technology, Pasadena, CA 92215, [4]Harvard-Smithsonian Center for Astrophysics, Cambridge, MA 02138, USA.

*To whom correspondence should be addressed. E-mail: ken@seismo.unr.edu

A deep earthquake swarm in late 2003 at Lake Tahoe, California (Richter Magnitude [M_L] < 2.2; depth 29-33 kilometer), was coeval with a transient displacement of 6 millimeters horizontally outward from the swarm and 8 millimeters upward measured at GPS station Slide Mountain (SLID) 18 km to the northeast. During the first 23 days of the swarm, hypocentral depths migrated at a rate of 2.4 millimeters/second up-dip along a 45 kilometer^2 structure striking N30°W and dipping 50°E. SLID's 20 millimeter/year transient velocity implies a lower bound of 200 nanostrain/year (parts per billion per year) on local strain rates, an order of magnitude greater than the 1996-2003 regional rate. The geodetic displacement is too large to be explained by the elastic strain from the cumulative seismic moment of the sequence suggesting an aseismic forcing mechanism. Aspects of the swarm and SLID displacements are consistent with lower-crustal magma injection under Lake Tahoe.

The 12–14 mm/yr of northwest directed motion of the Sierra Nevada mountain range in eastern California and western Nevada relative to stable North America represents about 20–25% of the Pacific-North America plate motion budget (*1*, *2*). At the latitude of Lake Tahoe, California-Nevada, much of this shear and extension is concentrated in the westernmost Great Basin, characterized at the surface by strike-slip and normal faulting. The eastern boundary of the Sierra Nevada mountain range is a geologically young transition marked by north-striking, east-dipping normal fault systems that account for Great Basin extension, the westward evolution of the Sierra Nevada Great Basin transition, and the consequent eastward collapse of the competent Sierra block. Paleozoic and Mesozoic roof pendants and Cretaceous granites in the region are overlain by Miocene to approximately 3 Ma volcanic rocks and by a distinct younger period, 1–2 Ma, of localized rhyolitic and basaltic magmatism (*3*).

The shallow crust in the California-Nevada border region near Lake Tahoe includes north-south striking normal faults and north-east and north-west striking strike-slip faults operating within east-west oriented regional extension (σ_3). This is a consequence of the near equivalence of the maximum and intermediate (σ_1 and σ_2) compressive stresses (*4*, *5*). The base of the seismogenic zone in the region varies locally from about 15–18 km (*6*). In the Lake Tahoe area no crustal earthquakes deeper than 20 km can be identified from over 25 years of monitoring.

In map view, the deep crustal sequence straddles the northwest shore of Lake Tahoe and defines a 7x5 km planar structure striking N30°W and dipping 50°NE between 29–33 km depth (Fig. 1; fig. S1). A total of 1611 earthquakes were located in the swarm (sum of the moment magnitude of all events is Mw 3.1), and the 1179 best located events are shown (see supporting online text). The swarm began with an M 0.0 event on 12 August 2003 and continued through 19 February 2004. Fifteen earthquakes on 31 December 2003 and 1 January 2004 marked the last days with more than 1 located event and the last events of the swarm (as of July 26, 2004) occurred on 5, 8, 12 and 20 January and 19 February 2004. Daily activity rates are peaked at times when the earthquake depths are shallower (Fig. 2, A and B). The final temporal concentration of seismicity began on 22 November and peaked with 88 earthquakes on 27 November (Fig. 2A). Seismograms of the deep events resemble shallow tectonic earthquakes near Lake Tahoe that have impulsive P-wave arrivals and high frequency waveforms. However, no Long-Period (LP) earthquakes, generally thought to result from magma movement in the crust, have been identified.

Hypocentral depths progressed from about 33 to 29 km depth (relative to the elevation of Lake Tahoe) by 3 September at a rate of 2.4 ± 0.6 mm/s (8.5 m/hr) up-dip along the imaged planar structure (Fig. 2B). The temporal and spatial depth distribution implies a source propagating up-dip that had reached its shallowest extent by 3 September, 23 days into the sequence (Fig. 2B). This is consistent with the leading edge of a volcanic dike intrusion where earthquakes

are triggered due to high-strain rates and localized stresses at the injection front (*7*, *8*).

An increase in the upper crustal seismicity (< 18 km depth) began about 2 months after initiation of the deep-crustal sequence (fig. S2) and continued through June 2004. The largest of the shallow events occurred on 3 June 2004: an MW 4.2 earthquake at a depth of 8.5 km, about 10 km north-northeast of the epicentral region of the deep swarm. Counting the 2004 event, the Nevada Seismological Laboratory catalog lists 8 earthquakes $M_L \geq 4.2$ since 1950 within 30 km of the center of North Lake Tahoe. The mean rate is one event this size or larger every 6–7 years. The Coulomb failure function on shallow faults was probably altered, consistent with the increase in shallow seismicity.

Magnitudes for the Tahoe swarm range from M_L –0.2 to 2.2 with a b-value of 2.0 (see supporting online text). b-values much greater than 1 are anomalous for upper crustal tectonic earthquakes but typical of volcanic regions (*9*, *10*). In the Long Valley volcanic area, (*11*) found b-values as high as 1.8 for upper crustal sequences associated with upper crustal volcanic processes.

Double-couple focal mechanism solutions have been determined for the 24 largest events (ML > 1.5) using a combination of P-wave first-motion polarities and P and S-wave amplitudes (fig. S3; see supporting online text). With one exception, all have a reverse faulting component. Most solutions are consistent with zones of weakness moved to failure by a maximum compressive stress oriented 225° and plunging 30° southwest (fig. S4). The maximum compressive stress (σ_1) is aligned approximately normal to the imaged structure, consistent with tensile failure along the northeast dipping structure (*7*). Among the reverse-faulting events, the T-axes strike northeast, but over wide range (fig. S4). This is in contrast to regional east-west oriented extension observed in upper crustal focal mechanisms and consistent with normal fault orientations near Tahoe (*12*, *4*). A possible explanation is that the stress field is locally perturbed by processes within the volume of the swarm.

A continuously-recording geodetic GPS station on the summit of Slide Mountain (SLID) is located horizontally 18 km away at N60°E from the center of the swarm region and 31 km from the center of the NE-dipping imaged planar structure at depth, nearly perpendicular to the plane. SLID is part of the 53-station BARGEN network, continuously operating since 1996 to investigate tectonic deformation in the Basin and Range Province (*13*, *2*). The same instrument design (including receiver, antenna, radome, and deep-anchored braced monument) has been implemented at all BARGEN stations in the region of SLID without changes since December 1999; therefore our geodetic analysis started at 1 January 2000, including data through 28 June 2004.

GPS data from SLID were processed with data from the 5 nearest BARGEN stations (UPSA, GARL, SHIN, GABB, TUNG; 99–184 km from SLID) in 24-hour batches using the GIPSY OASIS II software to produce a time series of 3-d precise point positions (longitude, latitude, and ellipsoidal height) relative to ITRF2000 (*14–16*). Each station coordinate time series was de-trended and then regionally filtered (*17*) by subtracting the mean time series from the 5 neighboring stations. Annual periodic signals were then removed (*18*), and finally 7-day averages were formed (Fig. 3). The estimated annual signals have a mean amplitude of 0.3 mm in horizontal components, and 0.9 mm in height. The weekly time series have a 1-s.d. scatter of 0.5 mm in horizontal components, and 2.1 mm in height, prior to 2003.5. The formal error bars have their scale adjusted to be consistent with this scatter (see supporting online text).

In contrast to neighboring BARGEN stations, all three SLID coordinates undergo episodic displacement starting 2003.5 and lasting 6 months, coeval with the deep crustal seismicity. The difference in mean coordinates between periods 2004.0-2004.5 and 2003.0-2003.5 were taken as displacement estimates, yielding 3.1 ± 0.2 mm northward, 4.9 ± 0.3 mm eastward, 7.9 ± 1.0 mm upward (1-s.d. errors). The SLID 2-d horizontal displacement of 5.8 mm is oriented N58°E, approximately in the direction of SLID relative to the source region, with the 3-d vector displacement of 9.8 mm aligned approximately normal to the planar structure at depth. In contrast, for the 5 neighboring stations the root mean square of estimated displacements is 0.4 mm for horizontal components, 0.7 mm for height, and 0.9 mm in total distance; which provides a realistic estimate of the total error in SLID's displacement, and is consistent to within 2 s.d. of the formal errors.

These results yield a transient change in velocity of SLID during 2003.5–2004.0 of 20 ± 2 mm/yr (12 ± 1 mm/yr horizontally). This in turn implies a lower bound on transient strain rates of 200 nstrain/yr (120 nstrain/yr horizontally) in the region between SLID and neighboring stations. These rates are several times higher than (and in addition to) the 1996–2003 regional strain rate of 30–40 nstrain/yr reported from BARGEN observations before the transient (*2*), and an order of magnitude greater than the estimated errors.

The extent of fault rupture is typically estimated from aftershock distributions. The area of the planar structure at depth (45 km^2), assuming a stress drop of 10 MPa (reasonable for upper crustal earthquakes), would cause a seismic moment equivalent to a moment magnitude (Mw) 6.0 and displacement of ~1 meter at the source. Reverse faulting on the imaged structure at depth (hanging wall up and to the southwest) would result in horizontal displacements at SLID up and to the southwest, so the horizontal component would be in the opposite direction to observations. Normal faulting,

on the other hand, although characteristic of the Lake Tahoe region, would result in a loss of elevation at SLID. A dilation mechanism can fit the geodetic data. Applying Okada's (*19*) model for a tensile crack at 30 km depth in the source region, a potency equivalent to a volume of 3.7 x 10^7 m^3, or volumetric moment equivalent of Mw 6.1, fits the SLID observations (see supporting online text). Since only one GPS station is available the source of the displacements at SLID cannot be uniquely determined. Mechanisms such as the introduction of fluids in the volume between the deep swarm and SLID or volumetric expansion of a potential source of magma below the deep crustal swarm could be developed to fit SLID motions.

The temporal correlation of SLID motions and deep seismicity strongly suggest the source of SLID displacements is spatially correlated with the earthquake swarm. SLID motions are not consistent with a shear dislocation but with dilation, or tensile failure, along the deep structure. Also, the progression of earthquake depths and stress field implied from earthquake focal mechanisms is consistent with other observations of dike intrusion (8). In addition, the high b-value of the Lake Tahoe sequence is most likely in response to high-strain rate driven rock failure typical of dike injection (*7*). The injection front of a propagating dike represents the temporal progression of earthquake depths, whereas the high frequency character of the events require brittle failure of rock at the crack tip. Also, tensile failure along east dipping structures would be consistent with east-west extension along the Great Basin Sierra Nevada transition near Lake Tahoe. High dilatational strains rates are inferred from GPS data in the Lake Tahoe region (Fig. 4). SLID deformation and the character of the earthquake swarm are consistent with magma injection. The volumetric source required to fit SLID observations would correspond to a ~1 meter thick dike over the area of the imaged structure at depth. Dipping eastward at 50°, the lower-crustal structure would project to the surface west of the Sierra Nevada Great Basin frontal fault system west of Lake Tahoe. However, if a Sierra Nevada Great Basin bounding structure, or structural zone, shallows eastward into the lower crust the event may have taken place near or within this structural boundary.

Periodic aseismic transient deformation in the Cascadia subduction zone is associated with deep crustal LP's (25-45 km depth), tremor like seismic signatures (*20*, *21*). Outside of subduction regions, however, deep brittle failure earthquakes are uncommon due the predominance of a brittle-ductile transition in the mid-crust and increased temperature with depth. Brittle failure at these depths requires localized high-strain rates that can result from magma injection. Deep earthquakes observed in the western Sierra foothills (*22*) may be in response to the same mechanism (Fig. 4). We suggest that this magmatic phenomenon should not be viewed as a likely precursor to volcanism, but rather as part of the tectonic cycle of lower crustal evolution, perhaps providing a mechanism to sustain crustal thickness and crustal strength in zones of extension.

References and Notes

1. T. Dixon, M. Miller, F. Farina, H. Wang, D. Johnson, D, *Tectonics* **19**, 24 (2000).
2. R. Bennett, B. Wernike, N. Niemi, A. Friedrich, and J.Davis, *Tectonics*, v.22, n.2, 31 (2003).
3. C. Henry, J. Faulds, (abstract) EarthScope/NSF Great Basin Symposium Lake Tahoe, California, June 21-23 (2004).
4. R. Schweickert, M. Lahren, K. Smith, J. Howle, *Tectonophys*., in press, (2004).
5. S. Wesnousky, C. Jones, *Geology* **22**, 1031, (1994).
6. Nevada Seismological Laboratory Historical Earthquake Catalog, accessible and searchable at http://www.seismo.unr.edu/Catalog/catalog-search.html.
7. A. Rubin, D. Pollard, *Geology* **16**, 413 (1988).
8.. M. Ukawa, H. Tsukahara, *Tectonophysics* **253**, p. 285 (1996).
9. McNutt, S. R., *International Handbook of Earthquake and Engineering Seismology, Part* Academic Press (2002).
10. V. Zobin, *Introduction to Volcanic Seismology*, Elsevier, (2003).
11. S. Wiemer, S. McNutt, M. Wyss, California, *Geophys. J. Int*., v. 134, 409 (1998).
12. G. Ichinose, J. Anderson, K. Smith, J. Anderson, *Seism. Soc. Am. Bull*. **93**, 61 (2003).
13. B. Wernicke, A. M. Friedrich, N. A. Niemi, R. A. Bennett, and J. L. Davis, *GSA Today 10* (*11*), 1—7,(2000).
14. J. Zumberge, M Heflin, D. Jefferson, M. Watkins, F. Webb, *J. Geophys. Res., 102*, 5005 (1997).
15. G. Blewitt, *J. Geophys. Res.Vol. 94*, No. B8, p. 10,187-10,283 (1989).
16. Z. Altamimi *et al*., *Am. Geophys. U*., Vol. 82, 273 (2001).
17. S. Wdowinski, Y. Bock, J. Zhang, P. Fang, and J., *J. Geophys. Res.*, **102**, 18,057- (1997).
18. G. Blewitt, G., D. Lavallee, *J. Geophys. Res*., Vol. 107 (B7), 10.1029/2001JB000570, (2002).
19. Y. Okada, *Bull. Seism. Soc. Am*., **75**, 1135 (1985).
20. H. Dragert, K. Wang, T. James, *Science* **292**, 1525, (2001).
21. G. Rogers, H. Dragert, *Science* **300**, 1942 (2003).
22. I. Wong, W. Savage, *Bull. Seism. Soc. Am*. **73**, 797 (1983).

23. The University of Nevada Reno seismic network in northern Nevada is operated under the U.S. Geological Survey National Earthquake Hazards Reduction Program with support from the State of Nevada. The GPS data analysis was funded by the Department of Energy, Yucca Mountain Project. The BARGEN GPS network is funded

by the National Science Foundation and the Department of Energy, with operational support from UNAVCO, Inc. The GIPSY OASIS II software and global GPS data products were provided by the Jet Propulsion Laboratory. We would like to thank Gary Oppliger for a review of the manuscript and Mark Coolbaugh for generating the regional strain map figure. Several stations in the Nevada K-12 seismic network, Storey County High School, Carson City High School, Douglas County High School, contributed phase arrival data for constraining earthquake locations in the lower-crustal swarm. We would like to thank 3 anonymous reviewers for their time and considerable effort in reviewing the manuscript.

Supporting Online Material
www.sciencemag.org/cgi/content/full/1101304/DC1
SOM Text
Figs. S1 to S4
References

9 June 2004; accepted 28 July 2004
Published online 5 August 2004; 10.1126/science.1101304
Include this information when citing this paper.

Fig. 1. Deep earthquake activity (> 20 km) in the Lake Tahoe California area, 2003– 2004, and location of GPS station SLID and faults with Holocene displacement (*8*). Red circles, N. Tahoe seismograph stations. Major east-dipping normal faults, TSFFZ: Tahoe-Sierra frontal fault zone; WTF: West Tahoe fault zone: NTFZ; North Tahoe fault zone: Cross-sectional view along strike, N30°W, of structure at depth.

Fig. 2. (**A**) Daily number of earthquakes; all located events. (**B**) Temporal progression of earthquake depths relative to 33 km depth along up-dip distance of lower-crustal structure. The dashed line is a rate of 2.4 mm/s from 12 August through 3 September 2003.

Fig. 3. GPS coordinate time series for SLID and neighboring stations in each of three component directions. Data displayed are 7-day averages with scaled formal error bars. Coordinate axes for SLID are extended to accommodate the signal, but the scale is the same for all stations. The scale of the height component is a factor of 3 greater than for the horizontal components to visually normalize the higher level of noise in height.

Fig. 4. Dilational strain map determined from GPS stations in the Sierra region. Solid symbols (•) are stations used in calculating dilational strain and circled symbols are BARGEN array stations. Best located events from the ANSS earthquake catalog between 20 and 50 km depth (□) are included.

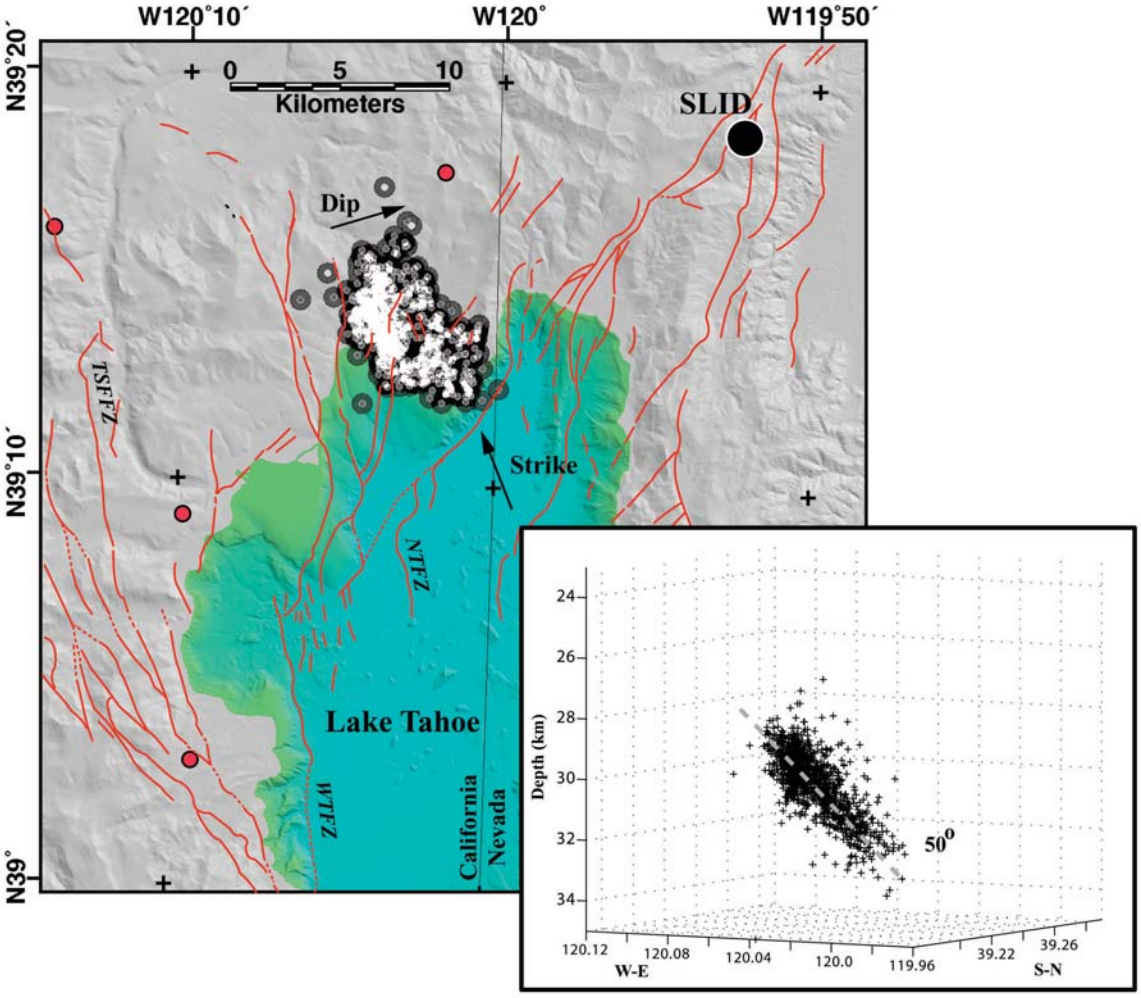
W120°10´
W120°
W119°50´
N39°20´
N39°10´
N39°
0
5
10
Kilometers
SLID
Dip
Strike
TSFZ
NTFZ
WTFZ
Lake Tahoe
California
Nevada
Depth (km)
24
26
28
30
32
34
50°
120.12
120.08
120.04
120.0
119.96
W-E
39.22
39.26
S-N

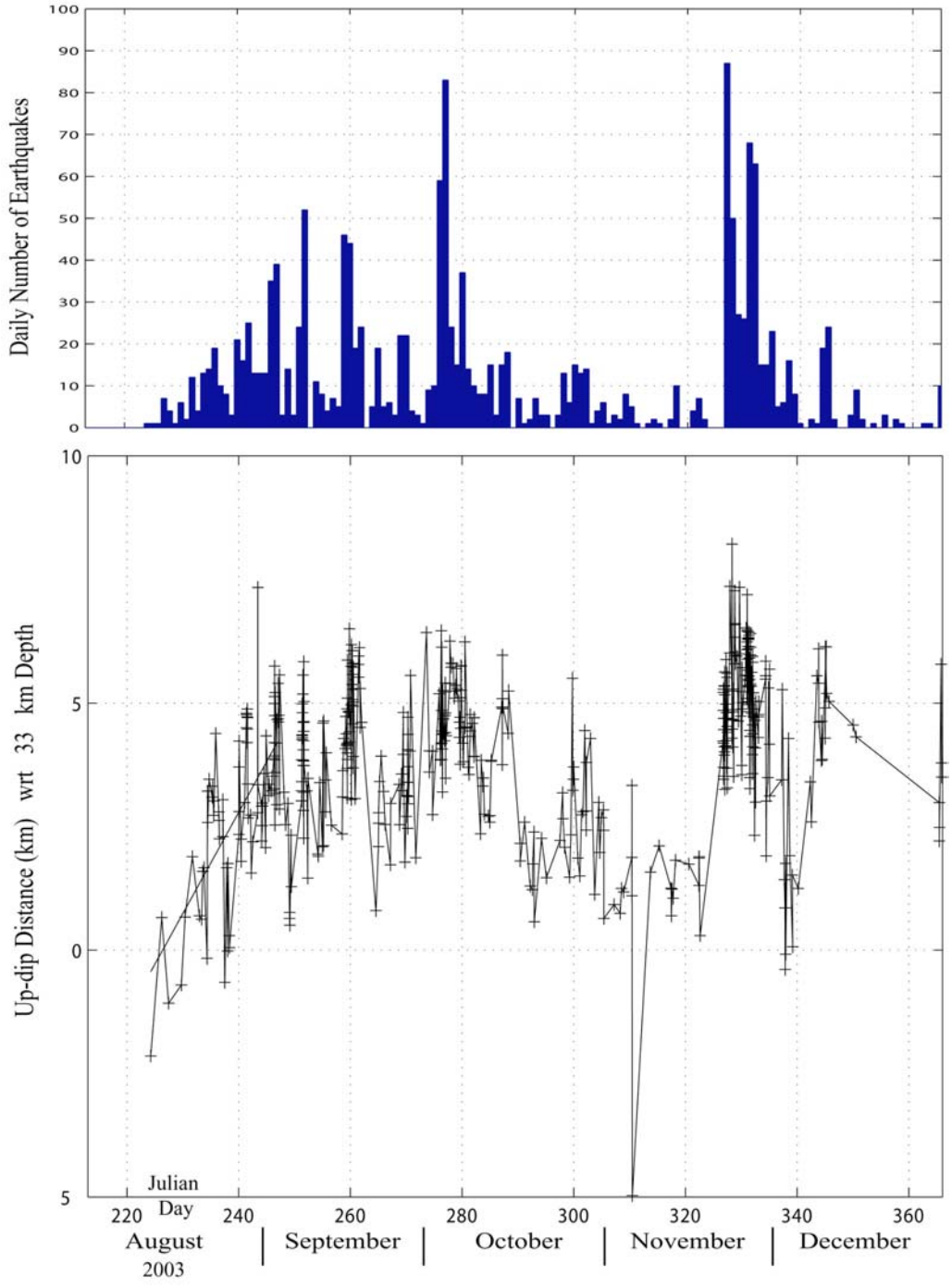
Daily Number of Earthquakes
100
90
80
70
60
50
40
30
20
10
0
Up-dip Distance (km) wrt 33 km Depth
10
5
0
5
Julian Day
220
240
260
280
300
320
340
360
August
2003
September
October
November
December

Figure 2

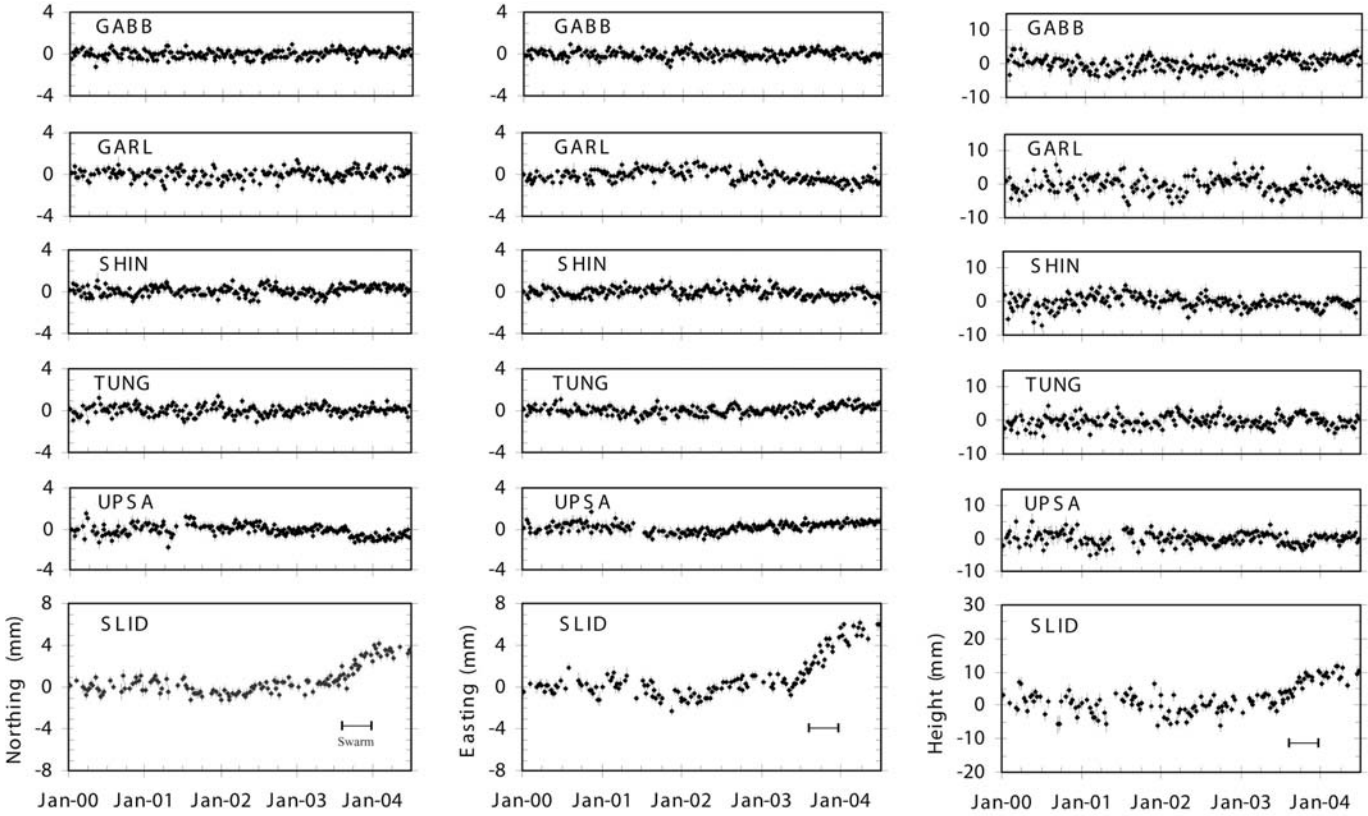
GABB
GARL
SHIN
TUNG
UPSA
SLID
Swarm
Northing (mm)
Easting (mm)
Height (mm)
Jan-00
Jan-01
Jan-02
Jan-03
Jan-04

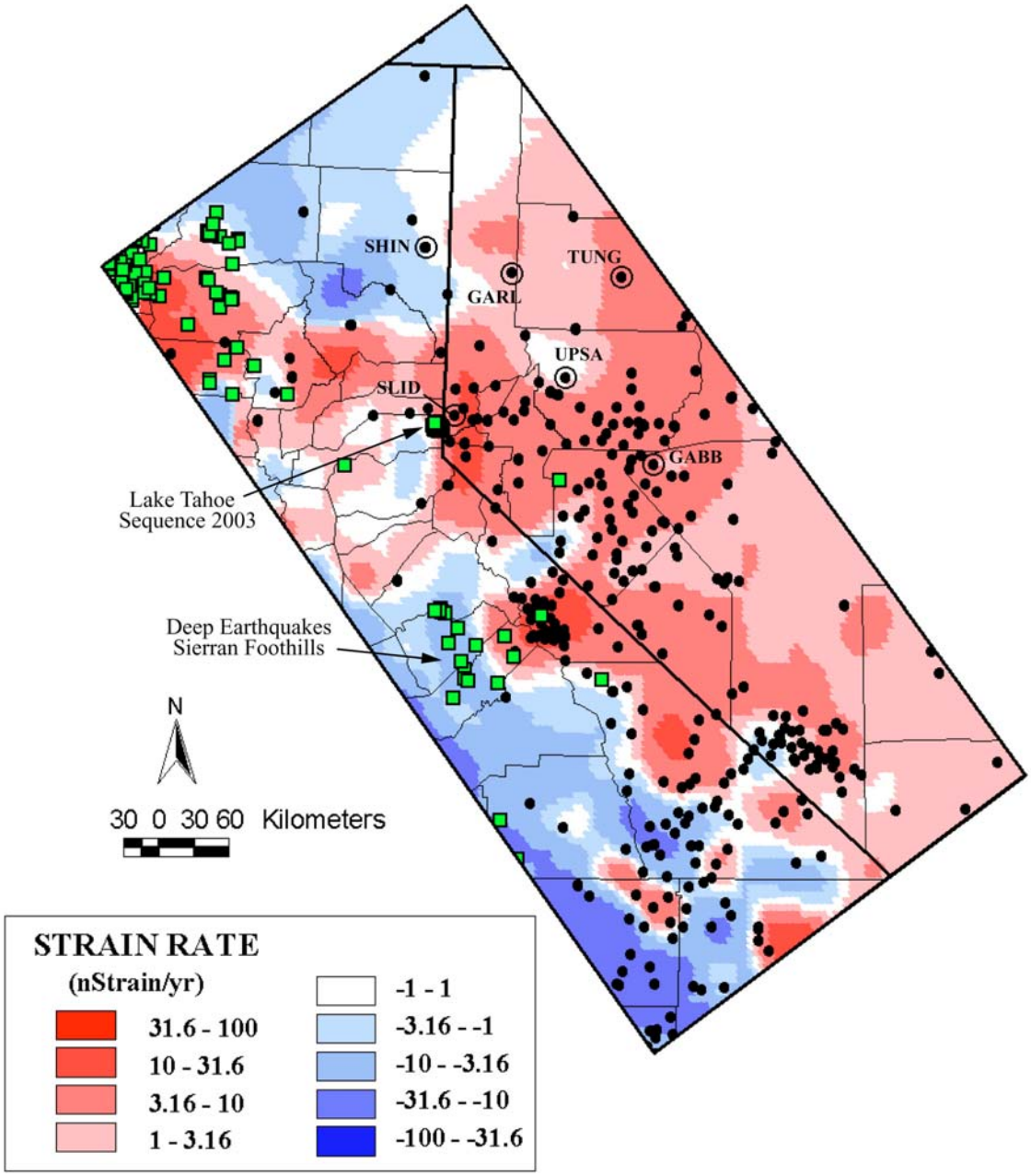
SHIN
TUNG
GARL
UPSA
SLID
GABB
Lake Tahoe
Sequence 2003
Deep Earthquakes
Sierran Foothills
N
30 0 30 60 Kilometers
STRAIN RATE
(nStrain/yr)
31.6 - 100
10 - 31.6
3.16 - 10
1 - 3.16
-1 - 1
-3.16 - -1
-10 - -3.16
-31.6 - -10
-100 - -31.6